

Spontaneous Nanoparticle Dispersal in Polybutadiene by Brush-forming End-Functional Polymers.

James M. Hart,¹ Solomon M. Kimani,^{1,2} Lian R. Hutchings,¹ Isabelle Grillo,³ Arwel V. Hughes⁴, Nigel Clarke,^{1,5} Vicky Garcia-Sakai,⁴ Sarah E. Rogers,⁴ Budhika Mendis⁶ and Richard L. Thompson.^{1,*}

1. Department of Chemistry, Durham University, Mountjoy Site, Durham, DH1 3LE, UK
2. Current address: Synthomer Limited, Central Road, Templefields, Harlow, CM20 2BH, UK
3. Institute Laue Langevin, Institut Laue-Langevin, 71 avenue des Martyrs, 38000 Grenoble, France
4. ISIS Pulsed Neutron Source, Rutherford Appleton Laboratories, Chilton, Didcot, OX11 0QX, UK
5. Department of Physics and Astronomy, The University of Sheffield, Hicks Building, Hounsfield Road, Sheffield, S3 7RH, UK
6. Department of Physics, Durham University, Mountjoy Site, Durham, DH1 3LE, UK

[*r.l.thompson@durham.ac.uk](mailto:r.l.thompson@durham.ac.uk)

KEYWORDS: Silica, nanocomposite, SANS, rheology, adsorption

A masterbatch additive for the enhanced dispersal of bare silica nanoparticles in polybutadiene is demonstrated using tetra-hydroxyl end-functional polybutadienes (“4OH-PBd”). Neutron reflectometry and SANS confirm the efficient end-adsorption of 4OH-PBd at a 1D silica interface, and silica particle interfaces of increasing complexity. SANS on well-defined model Stöber silica nanospheres in polybutadiene revealed spontaneous 4OH-PBd adsorption, forming a ‘shell’ around the silica nanospheres. Analysis using a core-shell fractal model system showed that the extent of adsorption and was consistent with the interfacial excess determined by NR. The utility of 4OH-PBd additives to disperse silica nanoparticles was explored rigorously for a range of compositions and additives. Successful silica nanoparticles dispersal was evident from a reduction in the correlation length of the largest structures in the mixture and increase in fractal dimension, ascribed to a breakdown of percolating nanoparticle aggregates to smaller, denser clusters. A critical surface concentration of 4OH-PBd is identified, which is necessary to inhibit particle-particle aggregation. Scaling theory analysis over four different molecular weights of 4OH-PBd and several concentrations indicates that the transition in silica dispersal coincides closely to the transition from ‘mushroom’ to ‘brush’ scaling of the adsorbed 4OH-PBd. Rheological testing on the same composites yielded a dramatic decrease in moduli with increasing 4OH-PBd : silica ratio, particularly at low frequencies, which is consistent with the breakdown of large aggregates evidenced by SANS. Additives of this type could significantly simplify the processing of nanocomposites by eliminating the need for prior functionalisation of the nanoparticles.

Composite and nanocomposite materials offer significant advantages over unfilled polymers, notably in mechanical, thermal and optical properties, with greater strength, resistance to heat and photodegradation being among these desirable properties. These benefits are perhaps best exemplified by the very successful use of filler particles in car tyres. Nevertheless, considerable challenges remain in simultaneously optimising different aspects of performance, such as durability, wet grip and energy efficiency. Energy efficiency is substantially compromised by strain softening (Payne) and hysteresis (Mullins) effects, which are prevalent in filled rubbers.¹⁻⁴ Re-

markably for this mature technology, there is still debate over the exact cause of reinforcement and associated phenomena such as energy dissipation, although it is apparent that the distribution of filler particles and their interactions with each other and the surrounding polymer are of central importance.

For other applications, controlling nanoparticle dispersion in polymers for magnetic inks and data storage is a current challenge⁵ and polymer reinforcement, e.g. with graphene-based fillers, requires control over the polymer-particle interface.⁶ Given these drivers, there is therefore

of considerable interest in controlling the dispersion and organisation of filler particles in rubbery polymers and the relationship between structure and performance.

It is established that modifying the surface of nanoparticles to render them more compatible with a polymer matrix is an important step towards achieving their dispersal. This analogous process is well known for colloidal solutions and the use of an adsorbed layer to achieve steric stabilisation has been documented since the 1970s⁷. For nanoparticle dispersal in polymers this approach to make nanocomposites is still a developing field. Notably, Corbierre *et al*⁸ report the use of thiol end-capped polymers to disperse gold nanoparticles. Successful dispersal required the matrix to wet the adsorbed stabilising layer, which necessitated either a low molecular weight matrix relative to the adsorbing polymer, or a relatively low grafting density such that some voids on the surface were present. As the formation of a percolating filler structure is thought to reinforce a composite, disruption of this process should cause in considerable changes of material properties⁹⁻¹⁰. Reports have noted the effects of structure formation and disruption on composite behaviour before. Jouault *et al*¹¹ have used SANS and rheology to explore the fractal properties of silica in PS homopolymer. Interestingly, they observed significant reinforcement at a silica volume fraction of 0.066, which is much lower than volume fraction required to make a continuous network. Baeza *et al*¹²⁻¹³ have also combined scattering and rheology to silica SBR (styrene butadiene rubber) nanocomposites. In the absence of polymer functionalization, other than terminal silanol groups on the SBR, small clustered aggregates with a fractal dimension of ~ 2.4 were observed. Using deuterium labelling and reactive functional groups, the same group demonstrated a reduction in aggregate size with grafting, which appeared to require a critical minimum grafting density.¹³

Methods such as rheology are excellent for the determination of macroscopic properties, however, there is little direct information gained about the microscopic phenomena. Neutron scattering, on the other hand, provides details about phenomena on the molecular to microscopic level, but the difficulty lies in linking these to macroscopic properties. The combination of neutron scattering and rheological techniques is therefore a powerful approach to study both the micro and macroscopic regimes to investigate the reinforcement of polymer nanocomposites and gain insight into underlying molecular phenomena. In this article we explore for the first time the dispersal of silica nanoparticles using a series of well-defined end-functional polymers of systematically varying molecular weight and composition. By linking neutron reflectometry to examine the structure of interfacially adsorbed layers to SANS, which is sensitive to nanoparticle distribution as well as the adsorbed layer structure, we isolate these factors and can resolve the impact of grafting density on nanoparticle dispersion. Finally, rheometry carried out on the same samples that were the subject of the SANS experiment provides the relationship between nanoscale dispersal and macroscopic properties.

Methods

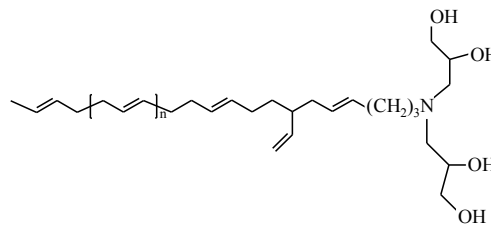


Figure 1: Chemical structure of the end functionalized polybutadiene (4OH-PBd)

Polymers

The synthesis and characterization methods have been previously reported,¹⁴ and will only be summarized here. Briefly, the end functional 1,4 polybutadiene, “4OH-PBd”, figure 1, used in these experiments was synthesized by anionic polymerization of butadiene, which was then end-capped with a tetrahydroxyl functional group. End-capping was carried out by a click reaction with at least 95% efficiency, as determined by NMR. Unfunctionalised perdeuterated polybutadiene was prepared by standard living anionic polymerization methods. Sample codes, molecular weight data and degree of end-capping data for the polymers used in this work are summarised in table 1.

Table 1: Summary of characteristics of 4OH end-functional and non-functional perdeuterated polybutadienes.

Sample code	M_n / kg.mol ⁻¹	M_w / kg.mol ⁻¹	% end-capping
4OH-PBd-5k	6.05	6.40	97
4OH-PBd-10k	9.80	10.3	96
4OH-PBd-15k	17.4	18.5	97
4OH-PBd-20k	22.5	23.6	95
d6-PBd-88k	88.0	90.6	n/a
d6-PBd-140k	138.0	140.8	n/a

Silica nanoparticles

Silica nanopowder (CAS #7631-86-9, lot 4830-012711) was purchased from Nanostructured and Amorphous Materials Inc., Houston, TX, USA and used as received. Additionally, silica spheres were prepared in-house from tetraethylorthosilicate using the Stöber process at room temperature¹⁵. Characterisation of these particles in aqueous solution by dynamic light scattering given as supporting information S.I.1 found the average radius was 45 nm (80-100 nm diameter), and subsequent TEM analysis, using a JEOL 2100F FEG TEM, confirmed that they were nearly monodisperse spheres (figure 2). TEM analysis of the nanopowder sample further confirmed the approximate size of the particles, quoted as 80 nm diameter,

which in this case are much less regular in shape. For clarity hereafter, we refer to the commercial nanopowder sample as ‘silica nanoparticles’ and the Stöber process sample as ‘silica nanospheres’. We note that for both silica materials, the average radius is more than 8 times the statistical step length of polybutadiene;¹⁶ therefore curvature effects on the adsorbed brush layer form are expected to be negligible.¹⁷

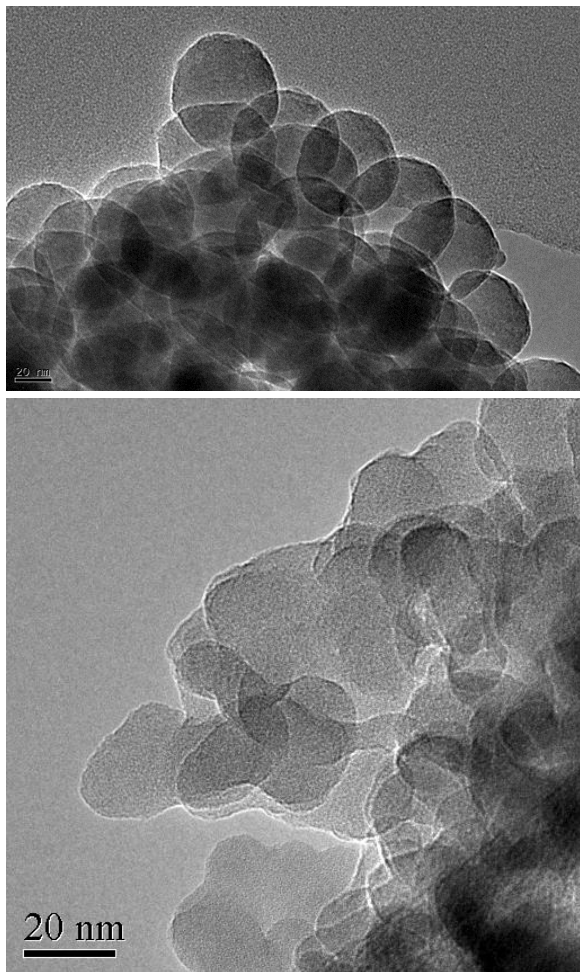


Figure 2: TEM image of Stöber silica nanospheres (top) and silica nanopowder (bottom). In both cases the scale bar corresponds to 20 nm.

Neutron Reflectometry (NR)

Thin (~75 nm) polybutadiene blend films were prepared by spin-casting from toluene solutions onto clean silicon blocks of 50 mm diameter and 5 mm thickness. Silicon blocks were thoroughly cleaned by first immersing in toluene, then drying, then immersing in permanganic acid to remove any last traces of organic impurities. The absence of organic contaminants was verified by ellipsometry, which confirmed the presence of a silicon oxide layer of 2-3 nm on the block surface. Here, this feature is important, because it means that the silicon-oxide block surface is the 1-dimensional analogue for the silica nanoparticles that are the main focus of this work. The func-

tional polymer, 4OH-PBd-20k, and matrix polymer, d₆-PBd-88K, were co-dissolved in the desired proportions to determine the average film composition. Neutron reflectometry was carried out on the SURF reflectometer, ISIS pulsed neutron and muon source, Rutherford Appleton Laboratories, Chilton, UK. Specular reflectivity was measured at incident angles of 0.25, 0.65 and 1.5 degrees, which enabled $R(Q)$ to be determined from $0.008 < Q / \text{Å}^{-1} < 0.35$, so covered the range from before the critical edge to a point at which the signal became indistinguishable from the background. Here, Q is the scattering vector, defined as $Q = (4\pi/\lambda) \sin \theta/2$, where λ is the de Broglie wavelength of the neutron and θ is the scattering angle.

Small-Angle Neutron Scattering (SANS)

A composite sample comprising 24:20:56 (w/w) ratio of Stöber silica spheres, 4OH-PBd-20k polymer, and perdeuterated 1,4 polybutadiene (d₆-PBd-140K); components were mixed by solvent casting in toluene. Sample environment was a quartz window cell, 13 mm diameter with a 1 mm spacer, at standard temperature and pressure. Measurements were performed on the SANS2D instrument at ISIS pulsed neutron and muon source. The incident beam was collimated to 6 mm with the front and rear detectors at 12m and 6m from the sample, respectively. This was to enable a large Q range ($0.0015 < Q / \text{Å}^{-1} < 0.85$) to be captured in a single measurement. Data were corrected and reduced to an absolute scale by comparison with a polystyrene standard using Mantid software¹⁸⁻¹⁹.

A range of similar samples for SANS scattering were also prepared at two loadings of commercial silica nanoparticles at (5 or 20 %(w/w)) and various loadings (1-16% w/w) of each 4OH-PBd additive (approximately 5k, 10k, 15k, and 20k) were used. The bulk matrix was perdeuterated polybutadiene d₆-PBd-88. Samples were characterized on the D11 diffractometer, Institut Laue Langevin, Grenoble, France using the same cell and conditions as for the SANS2D experiment. In order to capture a similar Q -range to SANS2d, three detector distances (1.2, 8 and 39 m) were used. Data were scaled to absolute values (partial differential scattering cross section / cm⁻¹) using the water cross-section with LAMP software.

Rheology

Following structural investigation by small-angle neutron scattering, the mechanical properties of the *same samples* were carried out by oscillatory shear rheometry using 8 mm parallel plate geometry. Initial strain sweeps were carried out to ensure that measurements were confined to the linear viscoelastic (LVE) region with a maximum strain of 1%. The primary mode of measurement was a series of frequency sweeps at various temperatures using an AR-2000 rheometer. Data was shifted to 20° C using the William-Landel-Ferry time-temperature superposition²⁰.

Results

1D Depth Profile

Specular neutron reflectivity data were fitted to scattering length density (SLD) profile using Motofit Software running on Igor.²¹ Constrained parameters were the upper and lower SLD of the polymer film components, which were held at 6.61 and $0.5 \times 10^{-6} \text{ \AA}^{-2}$ respectively.

The NR data and fit for a blended film comprising 16% 4OH-PBd-20k in d6-PBd-90k are shown in figure 3, along with the best fit that could be obtained for a simple 2 polymer layer model that allowed for a diffuse interface between the polymer layers. Data are presented as RQ^4 to remove the Q^{-4} dependence of $R(Q)$ over the main fitting region of interest. Even this relatively simple model, in which the key variables are the thickness and scattering length density of each layer and the width of the interface, captures the data well. The profile in scattering length density corresponding to this fit is shown in figure 4, and the corresponding volume fraction profile for the end-functional polymer is presented on a secondary axis for clarity. The NR results confirm the observation from our earlier work¹⁴ that the tetra-hydroxyl end functional polymer adsorbs very strongly to silica surfaces, and in fact our measurement suggests that almost all of the end functional polymer is adsorbed the substrate interface, and very little functional polymer is dispersed in the bulk of the film.

SANS data for the silica nanosphere dispersion were fitted with SASview software using a model of free and aggregated polydisperse core-shell particles and a Debye term to account for interchain scattering between deuterated and hydrogenous polybutadienes. Data and fit are shown in figure 5, and the fitting model has the general form given by equation 1

$$d\Sigma/d\Omega = I(Q) = bkgd + P(Q) + P(Q)*S(Q) + D(Q) \quad (1)$$

where *bkgd* is the background scattering, $P(Q)$ is the particle factor for core-shell spherical particles and $S(Q)$ is the structure factor and $D(Q)$ is the Debye scattering for free polymer chains.

Silica nanosphere filled PBd

Experimental SANS data obtained on Sans2d for 20% silica nanospheres in a mixture of multi-hydroxy end functional polybutadiene and perdeuterated polybutadiene are presented in figure 5. The strong scattering at very low Q is largely due to the silica particles (or their aggregates) which are likely to be coated with an adsorbed layer of 4OH-PBd-20k, and the weaker scattering at high Q ($>0.1 \text{ \AA}^{-1}$) is likely to be due to Debye scattering from intermixed deuterated and hydrogenous polybutadiene.

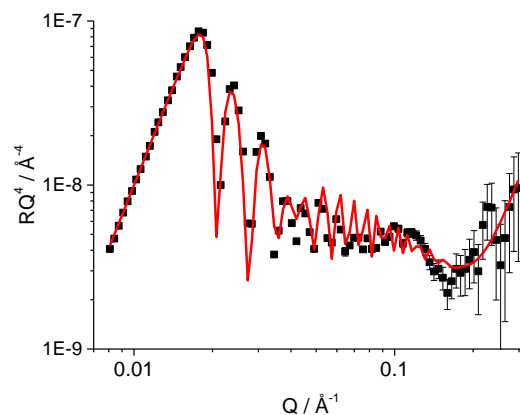


Figure 3: Neutron reflectivity data 16% 4OH-PBd-20k / dPBd-90k film on silica substrate (black) with fitted scattering curve (red)

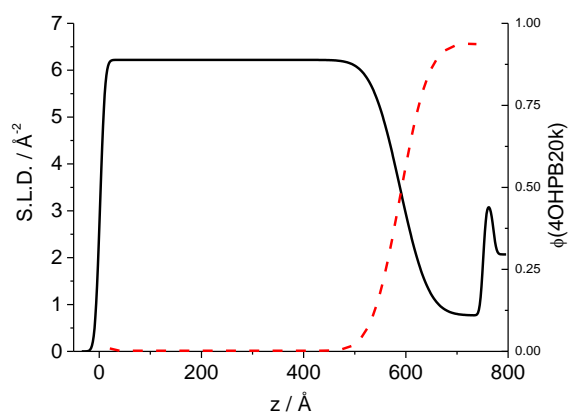


Figure 4: Calculated depth profiles for neutron scattering length density (black) and volume fraction of 4OH-PBd-20k (red) from the reflectivity data

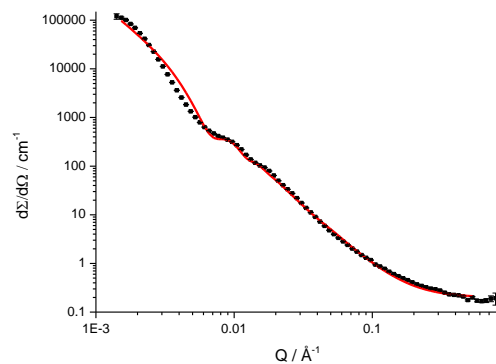


Figure 5: Small angle neutron scattering data for 24% Stober silica, 20% 4OH-PBd-20k, 56% d_6 -PBd-140k composite (black), curve (red) is for a combination of free particles and fractal aggregates with Debye and background terms.

The particle form factor is given by

$$P(Q) = \frac{scale}{V_s} \left[3V_c(\rho_c - \rho_s) \frac{(\sin(Qr_c) - Qr_c \cos(Qr_c))}{(Qr_c)^3} + 3V_s(\rho_s - \rho_{soln}) \frac{(\sin(Qr_s) - Qr_s \cos(Qr_s))}{(Qr_s)^3} \right]^2 \quad (2)$$

where ρ_c and ρ_s are the scattering length densities of the shell of adsorbed 4OH-PBd and silica sphere respectively, r_c , r_s , V_c and V_s are the radii and volumes of these components. The fractal structure factor has the form

$$S(Q) = \left[\frac{D\Gamma(D-1)\sin((D-1)\tan^{-1}(Q\xi))}{(Qr_c)^D \left(1 + \frac{1}{Q^2\xi^2}\right)^{\frac{D-1}{2}}} \right] \quad (3)$$

where ξ is the correlation length, Γ is the gamma function and D is the fractal dimension of the aggregate. The Debye factor has the usual form,

$$\frac{2(e^{-(QR_g)^2} + (QR_g)^2 - 1)}{(QR_g)^4} \quad (4)$$

where R_g is the radius of gyration associated with the blend polymer chains that are not adsorbed to the silica surface.

The core-shell form factor and fractal structure factor were used as calculated by Guiner and Teixeira, respectively²²⁻²³. Scattering length densities were held at the calculated values of $6.61 \times 10^{-6} \text{ \AA}^{-2}$ for the perdeuterated polybutadiene, $0.5 \times 10^{-6} \text{ \AA}^{-2}$ for the end functional polybutadiene, and $3.7 \times 10^{-6} \text{ \AA}^{-2}$ for the silica spheres. Silica core radii values, correlation length, and fractal dimension were varied with bounds to prevent unphysical results. Polymer shell thickness was tied between the particle sizes but allowed to vary otherwise. Scaling between the model sections was performed manually.

Silica nanoparticle dispersions

The same fractal scattering model was used to fit the SANS data for the silica nanoparticle dispersions, for which typical data and fits are shown in figure 6. For these samples the model captures the experimental data very well and the solid lines for the fits are almost obscured by the experimental data. SLD were constrained as previously, while particle radius, shell thickness, correlation length and fractal dimension were allowed to vary with reasonable bounds. Correlation length and particle

radius were found to decrease and the fractal dimension increased with increasing 4OH-PBd content. These changes in the model were observable as qualitative changes SANS data; namely the increasing bulge around 0.04 \AA^{-1} and the decrease in low Q slope with end functional polymer, which are apparent in figure 6. The fitted parameters for the nanoparticle dispersions are summarized in figure 3. Here, the sample code "XSi Y 4OH-PBd-Z k" indicates a mixture of X% (w/w) silica in Y% (w/w) 4OH-PBd of molecular weight Z kg/mol and 100-X-Y% (w/w) d₆-PB-88k. Plots of correlation length as a function of 4OH-PBd additive concentration are supplied as supporting information, S.I.2.

Table 2: SANS model parameters for Stöber silica nanospheres in a polybutadiene blend, corresponding to model fit in figure 5.

Parameter	Value
Radius, $r_s / \text{\AA}$	405 ± 61
Shell thickness $r_c - r_s / \text{\AA}$	173 ± 24
Fractal dimension D	2.20 ± 0.02
Correlation length $\xi / \text{\AA}$	4400 ± 3100

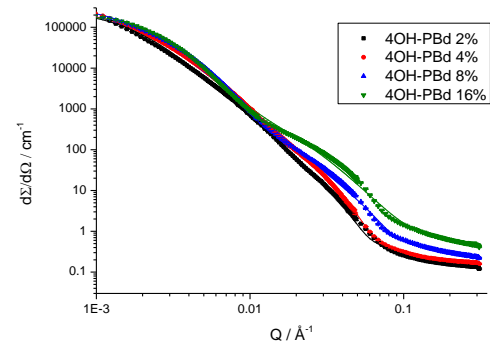


Figure 6: SANS data and fits for 5% (top) and 20% (bottom) silica nanoparticle samples with various 4OH-PBd-5k loadings

From the rheological tests, Figure 7, the combination of d₆-PBd-88K matrix and 4OH-PBd-20k polybutadienes results in an averaged modulus between them. The addition of 5% or 20% silica increases the storage modulus at both concentrations, while the loss modulus does not appear to be greatly affected in the 5% silica sample 4OH-PBd. The orders of magnitude increase in storage modulus is nonlinear with regard to the proportion of silica in the sample, in agreement with literature^{3-4, 24}; in other words there is significant reinforcement. The addition of end functional polymer induces a marked decrease in both the 5% and 20% composite sample moduli.

Table 3: Model parameters for SANS on silica nanoparticles in polybutadiene blends.

Sample	r_s / Å	r_c-r_s / Å	ξ / Å	D
20Si no 4OH-PBd	51.3	0.0	1160	2.20
20Si 2 4OH-PBd-5k	67.5	11.5	814	2.24
20Si 4 4OH-PBd-5k	37.7	22.0	426	2.45
20Si 8 4OH-PBd-5k	23.0	25.0	185	2.85
20Si 16 4OH-PBd-5k	29.1	13.4	197	2.69
20Si 4 4OH-PBd-10k	65.5	20.2	790	2.14
20Si 8 4OH-PBd-10k	34.0	28.0	195	2.85
20Si 16 4OH-PBd-10k	29.0	19.5	180	2.79
20Si 2 4OH-PBd-15k	73.9	16.5	883	2.29
20Si 4 4OH-PBd-15k	66.5	26.8	764	2.23
20Si 8 4OH-PBd-15k	46.4	50.0	388	2.36
20Si 16 4OH-PBd-15k	34.0	27.1	149	2.98
20Si 4 4OH-PBd-20k	64.6	35.3	721	2.22
20Si 16 4OH-PBd-20k	33.3	20.8	155	3.00
5Si 2 4OH-PBd-5k	29.0	23.5	553	2.80
5Si 4 4OH-PBd-5k	18.4	33.6	566	2.69
5Si 8 4OH-PBd-5k	21.3	9.9	553	2.77
5Si 16 4OH-PBd-5k	30.0	76.1	391	3.00
5Si 2 4OH-PBd-10k	29.9	23.1	620	2.76
5Si 4 4OH-PBd-10k	36.4	33.5	567	2.66
5Si 8 4OH-PBd-10k	26.7	13.5	431	2.83
5Si 16 4OH-PBd-10k	31.6	12.5	543	2.78
5Si 2 4OH-PBd-15k	26.6	33.0	651	2.77
5Si 4 4OH-PBd-15k	30.9	44.9	538	2.73
5Si 8 4OH-PBd-15k	34.0	33.1	331	2.93
5Si 16 4OH-PBd-15k	28.6	28.6	418	2.82
5Si 1 4OH-PBd-20k	48.7	33.1	1048	2.56
5Si 2 4OH-PBd-20k	31.0	40.9	608	2.79

Discussion

Interfacial structure

NR analysis revealed a hydrogenated 4OH-PBd-20k layer of 162 Å thickness and a sharp interface next to the silica substrate. The magnitude of the surface excess is in agreement with previous examinations of this polymer system by elastic recoil detection.¹⁴ Additionally, the neutron reflectometry can also resolve that the shape of the excess concentration profile is consistent with that of a brush-like layer.²⁵ If the adsorption of the end-functional polymer were due to the affinity of the entire chain, rather than just a single end-group to the silica surface, a

more exponentially decaying profile would be expected.²⁶⁻²⁸ This result gives us further confidence that the mode of adsorption is appropriate for a polymer chain required to enable dispersion of silica particles in polybutadiene, although the near exclusion of matrix from the adsorbed layer indicates that autophobic dewetting might be expected if similar grafting densities are achieved in the bulk.⁸ Although blends of deuterated and hydrogenous polybutadienes are known to phase separate at high molecular weight,²⁹ this cannot explain the observed result as the mean molecular weight of the deuterated and hydrogenous polybutadienes is orders of magnitude below this threshold.

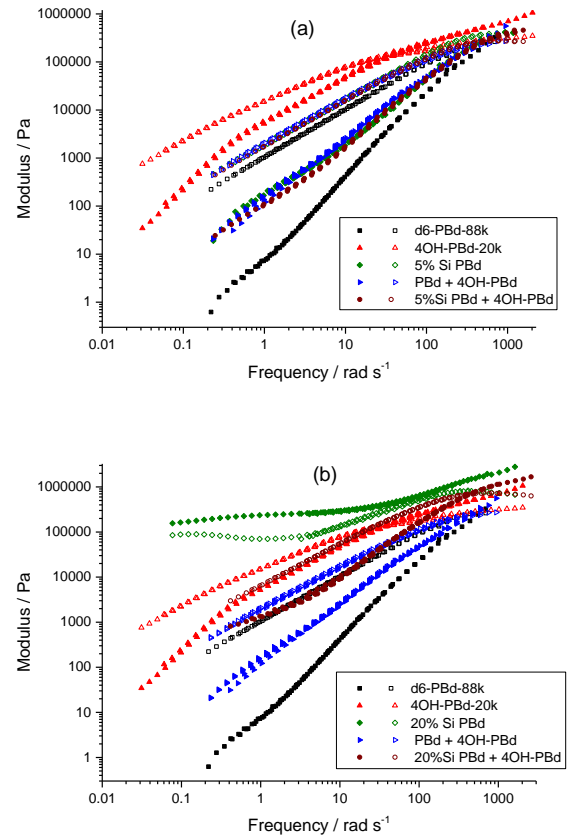


Figure 7: Storage (closed) and loss (open) moduli of WLF shifted frequency sweeps of samples 5% (a) and 20% (b) silica samples along with control measurements.

Bulk structure

Model silica nanosphere composites

The SANS data for this model nanocomposite system provides additional evidence to support the neutron reflectivity data as the shell thickness (table 2) calculated from r_c-r_s is in good agreement with the layer thickness measured by NR. Moreover, the spherical particle radius of 405 ± 61 Å obtained by SANS was consistent with the hydrodynamic radius (450 Å) determined by ancillary

dynamic light scattering experiments in aqueous dispersions of the nanospheres. The fractal core-shell scattering term suggests the presence of aggregated silica in the system with a fractal dimension of 2.2. The determined correlation length of the order of 4400 Å has a very large associated uncertainty. The correlation length is clearly finite, yet significantly larger than the individual particle size; therefore it indicates some degree of silica nanosphere association into small aggregates. The high uncertainty reported on the correlation length is likely due to a large range of aggregate sizes, possibly going beyond the range probed by the instrument. Given this variation in size, the aggregates are probably the result of ineffective dispersal of the starting silica nanospheres rather than from aggregation in solution, which would be expected to yield a narrower size distribution, and a larger apparent particle size determined by DLS. Overall this model provides a reasonable physical situation for the composite system in question with a mixture of free and aggregated particles producing the calculated scattered intensity. The result from this well-defined system justifies the use of a core-shell and fractal model for the analysis of other less defined silica composites.

Nanoparticle dispersions

There are several noticeable trends in the SANS data for the nanoparticle dispersion, summarized in table 3. Firstly, the absolute values of correlation length are significantly smaller than were recorded for the silica nanospheres, and all fall well within the range of the D₁₁ diffractometer. Furthermore, there is a notable decrease in correlation length with end functional polybutadiene content. This trend appears to be universal regardless of end functional chain length, though weaker in the 5% silica composite. Low polymer content and the bare silica control samples yield a fractal dimension of about 2.2; this is similar to the results for the nanosphere aggregates and to the reported value from reaction limited aggregation³⁰. The results in table 3 also show that there is a trend of increasing dimensionality toward 3 with the end-functional polymer content. At first glance an increase in fractal dimension yields a more compact arrangement; however it is important to couple this with the decrease in correlation length, ξ . The smaller more compact structure observed at high 4OH-PBd concentrations is likely the primary aggregate structure that forms the larger agglomerates observed at lower concentrations. This suggests a change from an aggregated cluster system toward a particulate system closer to hard sphere dispersion. Lin et al³¹ report that the fractal dimension of colloidal aggregates increases from 1.8 (or 1.86)³² to 2.10 ± 0.05 ³⁰ as the aggregation mechanism switches from diffusion limited to reaction limited. In other words, an activation energy barrier to aggregation, such as might be expected for the presence of a dense brush layer, should lead to more compact aggregates with a higher fractal dimension. Although the scaling exponents do not agree with our values, this is likely to arise from the fact that the silica particles are not aggregated from an initially homogeneous distri-

bution, but rather are being separated by a mixture of shearing during melt mixing and some degree of adsorption of the 4OH-PBd, when available. Nevertheless, the concept of a barrier to aggregation leading to smaller more condensed aggregations with a higher fractal dimension remains sound.

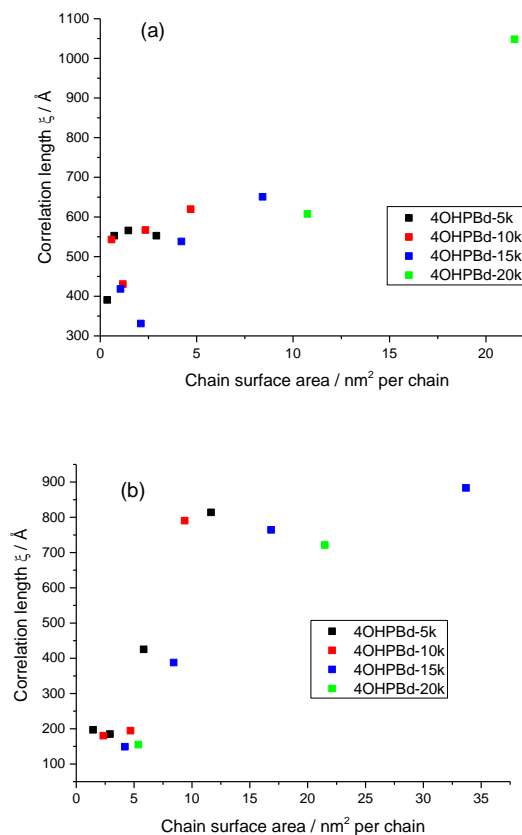


Figure 8: Correlation length versus calculated surface area per adsorbed chain for (a) 5% and (b) 20% silica nanoparticle dispersions

Further analysis was performed by the comparison of the data in regard to the chain surface area (figure 8). The available total surface area was calculated by treating the silica nanoparticles as ideal spheres with a set radius. The chain population was determined from the molecular weight, and was divided by the silica surface area to achieve the chain surface area. For the 20% silica composites, Figure 8(b), this method produces a noticeable step in correlation length at approximately 7.5 nm². This step is less visible in the 5% composite; however there is insufficient data to disprove its existence as most of the points are below the step in the 20% silica data.

This observed step in correlation length is likely due to the dispersion of the silica aggregates in the composite and the formation of a steric layer to stabilize the system. The correlation lengths at concentrations lower than the step, being of similar magnitude to that of the bare silica composite, 1160 Å, support this idea. The presence of the step itself suggests there is a critical surface concentration of the end functional chains that needs to be reached be-

fore the dispersal of the silica is energetically favourable, and that it is independent of chain length.

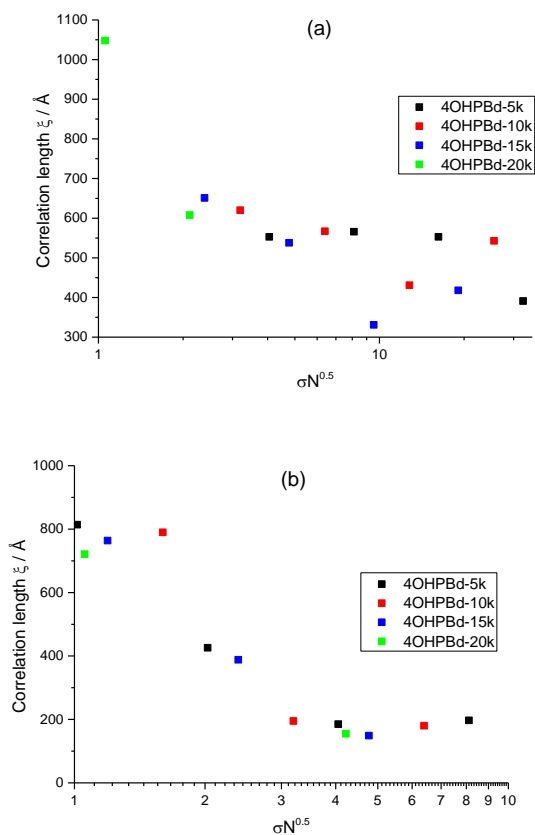


Figure 9. Correlation length versus normalised grafting density for (a) 5% and (b) 20% silica nanoparticle dispersions.

It is interesting to consider the step-like transition in behaviour in terms of the normalised grafting density of polymer brushes. Aubouy *et al* used scaling models to calculate a phase diagram for end-adsorbed polymer chains as a function of grafting density and molecular weight.³³ When the molecular weight of the matrix is equal to (or somewhat exceeds) that of the adsorbing species, no difference in adsorbed species brush height is expected with normalised grafting density until this reaches a value of $\sigma > N^{-1/2}$. Results for this analysis are presented in figures 9(a) and 9(b) for 5% and 20% silica respectively. Here, σ is the number of polymer chains adsorbed per unit area defined by the square of the statistical step length. Using the values of Aharoni¹⁶ of 9.6 Å for the statistical step length and 5.5 for the characteristic ratio of poly(1,4)butadiene, we obtain a value of 7.75 repeat units (mass 419 g/mol) for each statistical step. The critical value of σ is significant, because it corresponds to the boundary in the polymer brush scaling diagram at which the polymer brush first begins to become stretched. In other words, below this threshold value, it is possible to increase the number of polymer chains per unit area without perturbing the chain dimensions, so it

is reasonable to expect that bringing two particles into close contact is not accompanied by any entropically unfavourable effect on chain dimensions. Conversely at higher grafting densities, as two coated nanoparticles approach such that the particle – particle surface separation becomes comparable to the dimensions of the adsorbed 4OH-PBd layer, an entropic penalty associated with stretching the chains to accommodate their interdigitation would be incurred. This result is in agreement with the conclusions of Baeza *et al*¹³ in their study of grafted SBR silica composites, and significantly appears to hold true for several molecular weights of 4OH-PBd. The use of different molecular weights puts this result for correlation length versus normalised grafting density beyond doubt as it eliminates the uncertainty in the scaled grafting density that arises from the unknown prefactor in the brush phase diagram. Interestingly we find no evidence for aggregation based on autophobic dewetting as observed experimentally^{8, 34-35} and predicted in simulations, despite the NR results showing that there is almost complete exclusion of the matrix from the adsorbed brush layer apparent from the volume fraction profile in figure 4.

Also of note is that the correlation lengths of the dispersed 5% silica composites are substantially higher than those of the dispersed 20% composite. The reason for this difference could be due to the nature of the correlation length in the model and the concentration of the silica particles. The correlation length, ξ , is the upper limit to which the fractal distribution holds, and can be treated as a measure of aggregate size or a particle distribution correlation length. Bearing with the dispersal assumption, below the concentration threshold the silica is aggregated and the ξ measured relates to the aggregate size, resulting in a similar value between the data sets although with limited points. Once the silica is dispersed, the correlation length measured is that of a particle distribution and is inversely dependent on the concentration of particles. Hence a greater calculated correlation length in the 5% composites compared with the 20% composites may occur when the particles are dispersed.

Table 4: Saturated chain surface area for each 4OH-PBd estimated from interfacial excess measurements.

Polymer M_w / g mol ⁻¹	Effective surface thickness, z^* / nm ²	Calculated chain surface area / nm ² per chain
6400	9.4	1.26
10300	13	1.46
18500	15.7	2.17
23600	15.9	2.73

Saturated surface thicknesses have been measured from the previous investigation on 4OH-PBd's.¹⁴ The effective layer thickness was used to calculate the chain surface area in a saturated end functional layer. (table 4) The comparison of the D_{11} data with these values places the critical concentration about three to six times lower than the saturation value, which may explain why we do not encounter aggregation driven by autophobic dewetting in these materials. The observed trends can be described by three different regions of scattering behaviour dependent on the polymer concentration, visualized in Figure 10. The first region occurs at low 4OH-PBd concentrations where silica aggregate structures form due to the chains not being able to form adequate polymer layer for steric stability. After a critical polybutadiene surface concentration is reached steric stabilization of the silica particles can occur, resulting in the dispersal of the silica into a 'hard sphere' primary aggregate arrangement. This breakdown and dispersion of larger aggregates via steric stabilization is in agreement with recent results for carbon black and silica filler systems^{13, 36-38}. Eventually, saturation of the end functional layer results in the build-up of hydrogenated polybutadiene in the matrix, increasing Debye scattering as seen at $Q \sim 0.04 \text{ \AA}^{-1}$ in Figure 5a for 8% and 16% 4OH-PBd.

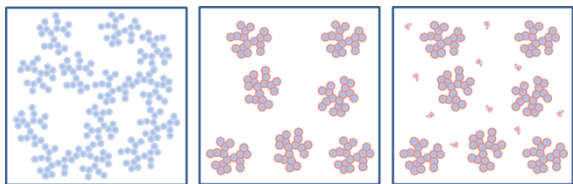


Figure 10: Depiction of a composite sample structure with increasing 4OH-PBd additive concentration, left to right

Rheometry of nanocomposites.

Before considering the filled polymer nanocomposites, we first examine the rheological behaviour of the pure matrix material dPBd-88k and that of the end functional polymer, 4OH-PBd-20k (figure 7). Despite having only about one quarter of the molecular weight than the matrix, the end-functional polymer has both higher moduli at low frequency and a slower terminal relaxation time, as evidenced by the lower cross-over frequency between G' and G'' . This is the first report of which we are aware concerning the rheology of multi-end functional polymers, but the result appears to be consistent with earlier SANS studies on related materials, which have shown that there can be a tendency to associate into star-like aggregates polymers.^{25, 39} As well as indicating aggregation for 100% end functional additive, which could not be measured with SANS due to the lack of a contrasting material, the intermediate modulus determined for the PBd + 4OH-PBd blend suggests that dilution with homopolymer does not disrupt the 4OH-PBd aggregates.

For filled rubbers containing both unfunctionalised matrix and 4OH-PBd, some averaging of moduli between the

deuterated and end functional polybutadiene is expected by standard rheological theories. Therefore, in the absence of any other effect, we would expect the replacement of dPBd-88k matrix with 4OH-PBd to increase the modulus of the material. The reduction in modulus observed with the addition of 4OH-PBd is therefore significant as it implies some change to the silica distribution.

Silica filler providing reinforcement to the polymer is well documented, though some contention remains over the exact reasons behind the phenomenon. The rheological results in light of the neutron scattering findings provide evidence for the percolating network theory of reinforcement. The increase in modulus between the 5% and 20% silica fractions without end functional polymer is much greater than a simple linear combination of moduli, suggesting some form of structure in the sample. The addition of the end functional polymer results in a sharp decrease in modulus for the 20% silica sample, while there is less change in the 5% silica sample. The decrease in terminal modulus with 'grafted' chains is a new feature, which appears to contradict the behaviour reported for styrene-butadiene/silica composites by Baeza et al.¹³ In this earlier study, the adsorbing polymer acted to separate the silica particles from dense, relatively discrete islands of silica towards a more expanded form in which the separation between structures was reduced. In our work, the starting point is that of a network, and the addition of adsorbing polymer disrupts this network. We note that the rheology in the presence of adsorbing polymers is qualitatively similar in each case.

The silica volume fraction in both the examined samples is well below the percolation threshold for spheres, 0.28, calculated by computer modelling⁴⁰. Similar reinforcement below this percolation threshold has been reported before, and has been partly attributed to the fractal structure of many filler particles resulting in percolation concentrations as low as $\phi \approx 0.033$ ⁴¹⁻⁴³. Because of this we theorize that the 20% silica is reinforced by the formation of silica aggregates structures running throughout the matrix, and that the breakup of aggregates with end functional polymer in the composite as seen by small angle neutron scattering decreases the reinforcement of the polymer matrix and the resultant elastic modulus. At 5% weight fraction a significant network cannot develop due to the scarcity of silica, thus there is less change with the addition of the 4OH-PBd as the system is already 'disperse', and appears to be offset by the higher modulus of the end functional material. This interpretation would support theories of matrix reinforcement based on the idea of a percolating network structure and at 5% silica loading suggests the presence of more localized aggregate structures that provide reinforcement rather than a large spanning network.

Conclusions

Through neutron reflectivity we find the preferential adsorption of end functionalized polybutadiene to silica surfaces in which the matrix is almost completely exclud-

ed from the adsorbed brush layer. Small angle neutron scattering yields evidence for the formation of fractal networks in the silica polybutadiene composites. Furthermore, the addition of end functionalized polybutadiene was found to spontaneously disperse unmodified silica aggregates to form a more open structure of individual particulates in which the correlation length of the fractal aggregates decreases and the fractal dimension increases. Despite the near exclusion of the matrix from the adsorbed polymer layer, we find no evidence for autophobic dewetting and instead find that the minimum grafting density for effective silica dispersal is unequivocally linked to the transition from mushroom to brush-like behaviour in the adsorbed layer structure. For our materials, the enhanced silica dispersal is accompanied by a change in material behaviour seen by the decrease in modulus in the samples and demonstrates the large effect a single functional group can have on total molecular and composite behaviour. The dispersion of silica and change in moduli provide evidence for percolating network theories of polymer composite reinforcement, and suggests that the reinforcement could be more localized than previously thought. We note that additives of this variety could significantly assist the processing of composite samples without the need for prior surface modification of the filler material.

Acknowledgement: We thank STFC for support of neutron scattering facilities at ISIS and ILL, and for support of JMH via Global Futures Scholarship ST/L502625/1. This work benefitted from the use of the SasView application, originally developed under NSF award DMR-0520547.

References:

- Meera, A. P.; Said, S.; Grohens, Y.; Thomas, S., Nonlinear Viscoelastic Behavior of Silica-Filled Natural Rubber Nanocomposites. *J. Phys. Chem. C* **2009**, *113* (42), 17997-18002.
- Merabia, S.; Sotta, P.; Long, D. R., A Microscopic Model for the Reinforcement and the Nonlinear Behavior of Filled Elastomers and Thermoplastic Elastomers (Payne and Mullins Effects). *Macromolecules* **2008**, *41* (21), 8252-8266.
- Payne, A. R., Dynamic properties of heat-treated butyl vulcanizates. *Journal of Applied Polymer Science* **1963**, *7* (3), 873-885.
- Payne, A. R., The dynamic properties of carbon black-loaded natural rubber vulcanizates. Part I. *Journal of Applied Polymer Science* **1962**, *6* (19), 57-63.
- Basly, B.; Alnasser, T.; Aissou, K.; Fleury, G.; Pecastaings, G.; Hadziioannou, G.; Duguet, E.; Goglio, G.; Mornet, S., Optimization of Magnetic Inks Made of Li(o)-Ordered FePt Nanoparticles and Polystyrene-block-Poly(ethylene oxide) Copolymers. *Langmuir* **2015**, *31* (24), 6675-6680.
- Kim, H.; Abdala, A. A.; Macosko, C. W., Graphene/Polymer Nanocomposites. *Macromolecules* **2010**, *43* (16), 6515-6530.
- Napper, D. H., Steric stabilization. *Journal of Colloid and Interface Science* **1977**, *58* (2), 390-407.
- Corbierre, M. K.; Cameron, N. S.; Sutton, M.; Laaziri, K.; Lennox, R. B., Gold nanoparticle/polymer nanocomposites: Dispersion of nanoparticles as a function of capping agent molecular weight and grafting density. *Langmuir* **2005**, *21* (13), 6063-6072.
- Maillard, D.; Kumar, S. K.; Fragneaud, B.; Kysar, J. W.; Rungta, A.; Benicewicz, B. C.; Deng, H.; Brinson, L. C.; Douglas, J. F., Mechanical Properties of Thin Glassy Polymer Films Filled with Spherical Polymer-Grafted Nanoparticles. *Nano Letters* **2012**, *12* (8), 3909-3914.
- Dorigato, A.; Dzenis, Y.; Pegoretti, A., Filler aggregation as a reinforcement mechanism in polymer nanocomposites. *Mechanics of Materials* **2013**, *61* (0), 79-90.
- Jouault, N.; Vallat, P.; Dalmás, F.; Said, S.; Jestin, J.; Boue, F., Well-Dispersed Fractal Aggregates as Filler in Polymer-Silica Nanocomposites: Long-Range Effects in Rheology. *Macromolecules* **2009**, *42* (6), 2031-2040.
- Baeza, G. P.; Genix, A. C.; Degrandcourt, C.; Petitjean, L.; Gummel, J.; Couty, M.; Oberdisse, J., Multiscale Filler Structure in Simplified Industrial Nanocomposite Silica/SBR Systems Studied by SAXS and TEM. *Macromolecules* **2013**, *46* (1), 317-329.
- Baeza, G. P.; Genix, A. C.; Degrandcourt, C.; Petitjean, L.; Gummel, J.; Schweins, R.; Couty, M.; Oberdisse, J., Effect of Grafting on Rheology and Structure of a Simplified Industrial Nanocomposite Silica/SBR. *Macromolecules* **2013**, *46* (16), 6621-6633.
- Kimani, S. M.; Hardman, S. J.; Hutchings, L. R.; Clarke, N.; Thompson, R. L., Synthesis and surface activity of high and low surface energy multi-end functional polybutadiene additives. *Soft Matter* **2012**, *8* (12), 3487-3496.
- Stöber, W.; Fink, A.; Bohn, E., Controlled growth of monodisperse silica spheres in the micron size range. *Journal of Colloid and Interface Science* **1968**, *26* (1), 62-69.
- Aharoni, S. M., On Entanglements of flexible and rodlike polymers. *Macromolecules* **1983**, *16* (11), 1722-1728.
- Kalb, J.; Dukes, D.; Kumar, S. K.; Hoy, R. S.; Grest, G. S., End grafted polymer nanoparticles in a polymeric matrix: Effect of coverage and curvature. *Soft Matter* **2011**, *7* (4), 1418-1425.
- Wignall, G. D.; Bates, F. S., Absolute calibration of small-angle neutron scattering data. *Journal of Applied Crystallography* **1987**, *20* (1), 28-40.
- Mantid. In *Manipulation and Analysis Toolkit for Instrument Data*, Mantid Project: 2013.
- Williams, M. L.; Landel, R. F.; Ferry, J. D., The Temperature Dependence of Relaxation Mechanisms in Amorphous Polymers and Other Glass-forming Liquids. *Journal of the American Chemical Society* **1955**, *77* (14), 3701-3707.
- Nelson, A., Co-refinement of multiple-contrast neutron/X-ray reflectivity data using MOTOFIT. *J. Appl. Crystallogr.* **2006**, *39*, 273-276.
- Teixeira, J., Small-angle scattering by fractal systems. *Journal of Applied Crystallography* **1988**, *21* (6), 781-785.
- Guinier, A.; Fournet, G., *Small-angle scattering of X-rays*. Wiley: New York, 1955.
- Gauthier, C.; Reynaud, E.; Vassoille, R.; Ladouce-Stelandre, L., Analysis of the non-linear viscoelastic behaviour of silica filled styrene butadiene rubber. *Polymer* **2004**, *45* (8), 2761-2771.

25. Ansari, I. A.; Clarke, N.; Hutchings, L. R.; Pillay-Narainan, A.; Terry, A. E.; Thompson, R. L.; Webster, J. R. P., Aggregation, Adsorption, and Surface Properties of Multiply End-Functionalized Polystyrenes. *Langmuir* **2007**, *23* (8), 4405-4413.
26. Bates, F. S.; Wignall, G. D.; Dierker, S. B., Phase behavior of amorphous binary mixtures of perdeuterated and normal 1,4-polybutadienes. *Macromolecules* **1986**, *19* (7), 1938-1945.
27. Schmidt, I.; Binder, K., Model-Calculations for Wetting Transitions in Polymer Mixtures. *Journal De Physique* **1985**, *46* (10), 1631-1644.
28. Zink, F.; Kerle, T.; Klein, J., Near-surface composition profiles in isotopic polymer blends determined via high-resolution nuclear reaction analysis. *Macromolecules* **1998**, *31* (2), 417-421.
29. Balsara, N. P., Physical Properties of Polymers Handbook. In *Physical Properties of Polymers Handbook*, Mark, J. E., Ed. American Institute of Physics: Woodbury, New York, 1996; pp 257-268.
30. Lin, M. Y.; Lindsay, H. M.; Weitz, D. A.; Ball, R. C.; Klein, R.; Meakin, P., Universal Reaction-Limited Colloid Aggregation. *Phys. Rev. A* **1990**, *41* (4), 2005-2020.
31. Lin, M. Y.; Lindsay, H. M.; Weitz, D. A.; Ball, R. C.; Klein, R.; Meakin, P., Universality in Colloid Aggregation. *Nature* **1989**, *339* (6223), 360-362.
32. Lin, M. Y.; Lindsay, H. M.; Weitz, D. A.; Klein, R.; Ball, R. C.; Meakin, P., Universal Diffusion-Limited Colloid Aggregation. *J. Phys.-Condes. Matter* **1990**, *2* (13), 3093-3113.
33. Aubouy, M.; Fredrickson, G. H.; Pincus, P.; Raphael, E., End-tethered chains in polymeric matrices. *Macromolecules* **1995**, *28* (8), 2979-2981.
34. Hasegawa, R.; Aoki, Y.; Doi, M., Optimum graft density for dispersing particles in polymer melts. *Macromolecules* **1996**, *29* (20), 6656-6662.
35. Sunday, D.; Ilavsky, J.; Green, D. L., A Phase Diagram for Polymer-Grafted Nanoparticles in Homopolymer Matrices. *Macromolecules* **2012**, *45* (9), 4007-4011.
36. Baeza, G. P.; Genix, A.-C.; Degrandcourt, C.; Petitjean, L.; Gummel, J.; Schweins, R.; Couty, M.; Oberdisse, J., Effect of Grafting on Rheology and Structure of a Simplified Industrial Nanocomposite Silica/SBR. *Macromolecules* **2013**, *46* (16), 6621-6633.
37. Gowney, D. J.; Mykhaylyk, O. O.; Derouineau, T.; Fielding, L. A.; Smith, A. J.; Aragra, N.; Lamb, G. D.; Armes, S. P., Star Diblock Copolymer Concentration Dictates the Degree of Dispersion of Carbon Black Particles in Nonpolar Media: Bridging Flocculation versus Steric Stabilization. *Macromolecules* **2015**.
38. Oberdisse, J.; El Harrak, A.; Carrot, G.; Jestin, J.; Boué, F., Structure and rheological properties of soft-hard nanocomposites: influence of aggregation and interfacial modification. *Polymer* **2005**, *46* (17), 6695-6705.
39. Kimani, S. M.; Thompson, R. L.; Hutchings, L. R.; Clarke, N.; Billah, S. M. R.; Sakai, V. G.; Rogers, S. E., Multihydroxyl End Functional Polyethylenes: Synthesis, Bulk and Interfacial Properties of Polymer Surfactants. *Macromolecules* **2014**, *47* (6), 2062-2071.
40. Rintoul, M. D.; Torquato, S., Precise determination of the critical threshold and exponents in a three-dimensional continuum percolation model. *Journal of Physics A: Mathematical and General* **1997**, *30* (16), L585.
41. Jouault, N.; Vallat, P.; Dalmás, F.; Said, S. r.; Jestin, J.; Boué, F. o., Well-Dispersed Fractal Aggregates as Filler in Polymer-Silica Nanocomposites: Long-Range Effects in Rheology. *Macromolecules* **2009**, *42* (6), 2031-2040.
42. Zhao, D.; Ge, S.; Senses, E.; Akcora, P.; Jestin, J.; Kumar, S. K., Role of Filler Shape and Connectivity on the Viscoelastic Behavior in Polymer Nanocomposites. *Macromolecules* **2015**.
43. Cassagnau, P., Payne effect and shear elasticity of silica-filled polymers in concentrated solutions and in molten state. *Polymer* **2003**, *44* (8), 2455-2462.

SYNOPSIS TOC The structural and rheological properties of silica nanoparticle dispersions in polybutadiene are dramatically altered when sufficient end functional polymer is present to create a stretched brush on the nanoparticle surfaces.

Insert Table of Contents artwork here

